Article

Dynamic complexity in a discrete-time predator-prey system with Holling type I functional response: Gompertz growth of prey population

Sarker Md. Sohel Rana
University of Dhaka, Dhaka 1000, Bangladesh
E-mail: srana.mthdu@gmail.com

Received 16 March 2020; *Accepted 25 April 2020*; *Published 1 December 2020*

Abstract
We consider a discrete-time predator-prey system with Holling type I functional response and Gompertz growth of prey population to study its dynamic behaviors. We algebraically show that the predator-prey system undergoes a flip bifurcation (FB) and Neimark-Sacker bifurcation (NSB) in the interior of $\mathbb{R}^2_+$when one of the model parameter crosses its threshold value. We determine the existence conditions and direction of bifurcations by using the center manifold theorem and bifurcation theorems. We present numerical simulations to illustrate theoretical results which include the bifurcation diagrams, phase portraits, appearing or disappearing closed curves, periodic orbits, and attracting chaotic sets. In order to justify the existence of chaos in the system, maximum Lyapunov exponents (MLEs) and fractal dimension (FD) are computed numerically. Finally, chaotic trajectories have been controlled by applying feedback control method.

Keywords predator-prey system; Gompertz growth; bifurcations; Lyapunov exponents; feedback control.

Computational Ecology and Software
ISSN 2220-721X
URL: http://www.iaees.org/publications/journals/ces/online-version.asp
RSS: http://www.iaees.org/publications/journals/ces/rss.xml
E-mail: ces@iaees.org
Editor-in-Chief: WenJun Zhang
Publisher: International Academy of Ecology and Environmental Sciences

1 Introduction

In ecological systems, the most significant studied theme is the interaction between predator and prey species. Many mathematical models have been developed to interpret and analyze qualitative behaviors of such systems. One can describe the dynamics of population growth if the functional behavior of growth rate is known. Different predator-prey models can be found in the literature (May, 1974; Freedman, 1980; Berryman, 1992). The simplest mathematical model describing a predator-prey interaction is the following well-known Kolmogorov type predator-prey model with Holling type I functional response:

$$\begin{aligned} \dot{x} &= g(x,K) - \alpha xy \\ \dot{y} &= \beta xy - dy \end{aligned} \tag{1}$$

where $g(x,K) = rx\left(1-\frac{x}{K}\right)$; x and y stand densities of prey and predator, respectively;

$r, K, \alpha, \beta,$ and d are all positive constants that stand for intrinsic growth rate of the prey, the carrying capacity of the prey, capturing rate of prey, conversion rate of predator, and the mortality rate of the predator, respectively. In (1), prey grows logistically if predator is absent. The qualitative analysis of solutions for system (1) is well established (Freedman, 1980; May, 1974). To investigate the dynamics of a community comprising of population of various interacting species, Gompertz (1825) developed an alternative expression for the prey birth rate which is similar in effect to logistic growth: $g(x, K) = rx \ln\left(\frac{K}{x}\right)$.

Though most predator-prey theories are based on continuous models governed by differential equations, in recent year, a lots of exploratory works have recommend that if population size is small, or population generations are relatively discrete (nonoverlapping), studies on discrete predator-prey model are more appropriate as it shows richer and very complex dynamics than the corresponding continuous model. Besides, for insects with non-overlapping generations, predator-prey system can be modeled in a discrete-time form and numerical computation also requires to discretize a continuous-time model (He and Lai, 2011; He and Li, 2014; Rana, 2015, 2017, 2019; Liu and Cai, 2019; Zhao et al., 2016; Zhao et al., 2017). These researches found many complex properties including attracting fixed point, stable orbits, periodic, quasi-periodic and non-periodic orbits through the possibility of flip and Neimark-Sacker bifurcations which had been derived either by numerically or by normal form and center manifold theory.

In this paper, we consider the following predator-prey system with Gompertz growth of prey:

$$\begin{aligned} \dot{x} &= rx \ln\left(\frac{K}{x}\right) - \alpha xy \\ \dot{y} &= \beta xy - dy \end{aligned} \tag{2}$$

Forward Euler scheme with integral step size δ is applied to system (2) to obtain following two-dimensional discrete system:

$$\begin{pmatrix} x \\ y \end{pmatrix} \mapsto \begin{pmatrix} x + \delta\left[rx \ln\left(\frac{K}{x}\right) - \alpha xy\right] \\ y + \delta[\beta xy - dy] \end{pmatrix} \tag{3}$$

Our aim of this study is to see how model parameters affect on the dynamics of system (3).In the discrete predator-prey system, the flip and NS bifurcation bifurcations are the main mechanisms to produce complex dynamics and cause the system to jump from stable to unstable states and trigger a route to chaos via periodic and quasi-periodic states. We analyze systematically the existence condition of these two bifurcationsin the interior of $\mathbb{R}^2_+$by using bifurcation theory and center manifold theory (Kuzenetsov, 1998).

This paper is organized as follows. Section 2 presents the existence condition for fixed points of system (3) and their stability criterion. The direction of bifurcation for system (3) under certain parametric condition are determined in Section 3. The diagrams of bifurcation, phase portraits, maximum Lyapunov exponents and Fractal dimensions of the system (3) for one or more control parameters are presented in Section 4 by implementing numerical simulations. In Section 5, we apply the feedback control method to stabilize chaotic unstable chaotic trajectories. Finally a short discussion is carried out in Section 6.

2 Existence Conditions and Stability Analysis of Fixed Points

2.1 Fixed points and their existence

The model system (3) possesses the following two fixed points for all permissible parameters value:

i. The axial fixed point $E_1(K,0)$. Biologically it means that the prey population reaches in the carrying capacity if predators are absent,

ii. The coexistence fixed point $E_2\left(x^* = \frac{d}{\beta}, y^* = -\frac{r\,\mathrm{Log}\left(\frac{K\beta}{d}\right)}{\alpha}\right)$. It exists and unique if $\beta > \frac{d}{K}$.

2.2 Dynamical behavior: stability analysis

We analyze local stability of system (3) at each fixed points by computing the magnitude of eigenvalues of Jacobian matrix evaluated at fixed point $E(x,y)$. The Jacobian matrix of system (3) around fixed point $E(x,y)$takes the form

$$J(x,y) = \begin{pmatrix} 1 - r\delta - y\alpha\delta + r\delta\mathrm{Log}\left(\frac{K}{x}\right) & -x\alpha\delta \\ y\beta\delta & 1 - d\delta + x\beta\delta \end{pmatrix} \quad (4)$$

Let $J(x,y) = (j_{mn}), m,n = 1,2$ (5)

Then the characteristic equation of matrix J is

$\lambda^2 + p(x,y)\lambda + q(x,y) = 0$ (6)

where $p(x,y) = -trJ = -(j_{11} + j_{22})$ and $detJ = j_{11}j_{22} - j_{12}j_{21}$.For stability conditions of fixed points, Jury's criterion (Elaydi, 1996) has been applied.

At $E_1(K,0)$, the Jacobian matrix (6) can be obtained as

$J(E_1) = \begin{pmatrix} 1 - r\delta & -K\alpha\delta \\ 0 & 1 - d\delta + K\beta\delta \end{pmatrix}$.

The eigenvalues of $J(E_1)$ are $\lambda_1 = 1 - r\delta$ and $\lambda_2 = 1 - d\delta + K\beta\delta$.

Proposition 2.1 *For the boundary fixed point $E_1(K,0)$, the following topological classification true*

a. *if $\beta < \frac{d}{K}$ then $E_1$is a sink if $0 < \delta < min\left\{\frac{2}{r}, \frac{2}{d-K\beta}\right\}$; source if $\delta > max\left\{\frac{2}{r}, \frac{2}{d-K\beta}\right\}$; . non-hyperbolic if $\delta = \frac{2}{r}$ or $\delta = \frac{2}{d-K\beta}$.*

b. *if $\beta > \frac{d}{K}$ then $E_1$is a source if $\delta > \frac{2}{r}$; saddle if $\delta < \frac{2}{r}$; non-hyperbolic if $\delta = \frac{2}{r}$.*

c. *if $\beta = \frac{d}{K}$ then $E_1$is always non-hyperbolic.*

It is obvious that when $\delta = \frac{2}{r}$ or $\delta = \frac{2}{d-K\beta}$, then one of the eigenvalues of $J(E_1)$is -1 and the other is not equal to ± 1. Therefore, a flip bifurcation can occur if parameters change in small neighborhood of $FB^1_{E_1}$ or $FB^2_{E_1}$:

$FB^1_{E_1} = \left\{(r,K,\alpha,\beta,d,\delta) \in (0,+\infty): \delta = \frac{2}{r}, \delta \neq \frac{2}{d-K\beta}, \beta < \frac{d}{K}\right\}$,

or$FB^2_{E_1} = \left\{(r,K,\alpha,\beta,d,\delta) \in (0,+\infty): \delta = \frac{2}{d-K\beta}, \delta \neq \frac{2}{r}, \beta < \frac{d}{K}\right\}$.

At $E_2(x^*,y^*)$, the Jacobian matrix (6) can be obtained as

$$J(E_2)=\begin{pmatrix} 1-r\delta & -\dfrac{d\alpha\delta}{\beta} \\ \dfrac{r\beta\delta\ \mathrm{Log}\left(\frac{K\beta}{d}\right)}{\alpha} & 1 \end{pmatrix}$$

where $trJ_{E_2}=2-r\delta$,and $detJ_{E_2}=1-r\delta+rd\delta^2\mathrm{Log}\left(\frac{K\beta}{d}\right)$.

Applying Jury's conditions, the fixed point E_2 is linearly asymptotically stable if and only if

$1+trJ_{E_2}+detJ_{E_2}>0$,
$1-trJ_{E_2}+detJ_{E_2}>0$,
$detJ_{E_2}-1<0$.

Let $\mathrm{A}_1=rd\ \mathrm{Log}\left(\frac{K\beta}{d}\right)$,$\mathrm{A}_2=-r$,$\mathrm{A}_3=4$,and $L=A_2^2-A_1A_3$.We state following Proposition about stability criterion of E_2.

Proposition 2.2 *Suppose $\beta>\frac{d}{K}$. Then the fixed point $E_2(x^*,y^*)$ of system (3) is a*

i. sink if one of the following conditions holds

(i.1) $L\geq 0 \quad and \quad \delta<\frac{-A_2-\sqrt{L}}{A_1}$;

(i.2) $L<0 \quad and \quad \delta<-\frac{A_2}{A_1}$;

ii. source if one of the following conditions holds

(ii.1) $L\geq 0 \quad and \quad \delta>\frac{-A_2+\sqrt{L}}{A_1}$;

(ii.2) $L<0 \quad and \quad \delta>-\frac{A_2}{A_1}$;

iii. non-hyperbolic if one of the following conditions holds

(iii.1) $L\geq 0 \quad and \quad \delta=\frac{-A_2\pm\sqrt{L}}{A_1};\ \delta\neq-\frac{2}{A_2},-\frac{4}{A_2}$

(iii.2) $L<0 \quad and \quad \delta=-\frac{A_2}{A_1}$;

iv. saddle if otherwise.

From Proposition 2.3, we see that two eigenvalues of $J(E_2)$ are $\lambda_1=-1$ and $\lambda_2\neq\mp1$ if condition (iii.1) holds. If (iii.2) is true, then the eigenvalues of $J(E_2)$ are complex having magnitude one.

Let

$FB_{E_2}^1=\left\{(r,K,\alpha,\beta,d,\delta)\in(0,+\infty):\delta=\frac{-A_2-\sqrt{L}}{A_1},\ L\geq 0,\delta\neq-\frac{2}{A_2},-\frac{4}{A_2}\right\}$, or

$$FB_{E_2}^2=\left\{(r,K,\alpha,\beta,d,\delta)\in(0,+\infty):\delta=\frac{-A_2+\sqrt{L}}{A_1},\qquad L\geq 0,\delta\neq-\frac{2}{A_2},-\frac{4}{A_2}\right\}.$$

Then system (3) experiences a flip bifurcation around fixed point E_2 if parameters vary in small vicinity of either set $FB_{E_2}^1$ or set $FB_{E_2}^2$.

Also let

$$NSB_{E_2} = \left\{(r, K, a, \alpha, \beta, d, \delta) \in (0, +\infty): \delta = -\frac{A_2}{A_1}, \qquad L < 0\right\},$$

Then if the parameters change around the setNSB_{E_2}, system (3) experience a NS bifurcation atE_2.

3 Direction and Stability Analysis of Bifurcation

In this section, we will pay attention to determine the direction and stability of flip and NS bifurcations of system (3) around E_2 by using center manifold theory. We set δ as a real bifurcation parameter.

3.1 Flip bifurcation

We take parameter $(r, K, \alpha, \beta, d, \delta)$ arbitrarily locate in $FB^1_{E_2}$. For the case of $FB^2_{E_2}$, one can do similar reasoning. Consider the system (3) at the fixed point $E_2(x^*, y^*)$ parameters lie in $FB^1_{E_2}$.

Let$\delta = \delta_F = \frac{-A_2 - \sqrt{L}}{A_1}$, then the eigenvalues of $E_2(x^*, y^*)$ are $\lambda_1(\delta_F) = -1$ and $\lambda_2(\delta_F) = 3 + \mathrm{A}_2\delta_F$.

In order for $|\lambda_2(\delta_F)| \neq 1$, we have

$$\mathrm{A}_2\delta_F \neq -2, -4 \tag{7}$$

We assume the transformation $\tilde{x} = x - x^*$, $\tilde{y} = y - y^*$ and write $A(\delta) = J(x^*, y^*)$. Then we shift the fixed point (x^*, y^*) of system (3) to the origin. After Taylor expansion, system (3) reduces to

$$\begin{pmatrix}\tilde{x}\\ \tilde{y}\end{pmatrix} \to A(\delta)\begin{pmatrix}\tilde{x}\\ \tilde{y}\end{pmatrix} + \begin{pmatrix}F_1(\tilde{x}, \tilde{y}, \delta)\\ F_2(\tilde{x}, \tilde{y}, \delta)\end{pmatrix} \tag{8}$$

where $X = (\tilde{x}, \tilde{y})^T$is the vector of the transformed systemand

$$\begin{aligned} F_1(\tilde{x}, \tilde{y}, \delta) &= \frac{1}{2}\left(-2\tilde{x}\tilde{y}\alpha\delta - \frac{r\tilde{x}^2\delta}{x^*}\right) + \frac{1}{6}\frac{r\tilde{x}^3\delta}{x^{*2}} + O(\| X \|^4)\\ F_2(\tilde{x}, \tilde{y}, \delta) &= \tilde{x}\tilde{y}\beta\delta + O(\| X \|^4) \end{aligned} \tag{9}$$

The system (8) can be expressed as

$$X_{n+1} = AX_n + \frac{1}{2}B(X_n, X_n) + \frac{1}{6}C(X_n, X_n, X_n) + O(\| X_n \|^4)$$

where $B(x, y) = \begin{pmatrix}-\frac{rx_1y_1\delta}{x^*} - \alpha\delta(x_2y_1 + x_1y_2)\\ \beta\delta(x_2y_1 + x_1y_2)\end{pmatrix}$ and $(x, y, u) = \begin{pmatrix}\frac{ru_1x_1y_1\delta}{x^{*2}}\\ 0\end{pmatrix}$ are symmetric multi-linear vector functions of $x, y, u \in \mathbb{R}^2$and $\delta = \delta_F$. In coordinates, we have

$B_{\mathrm{i}}(x, y) = \sum_{j,k=1}^{2} \frac{\delta^2 F_{\mathrm{i}}(\xi, \delta)}{\delta\xi_j\delta\xi_k}\Big|_{\xi=0} x_jy_k$ and $C_{\mathrm{i}}(x, y, u) = \sum_{j,k,l=1}^{2} \frac{\delta^2 F_{\mathrm{i}}(\xi, \delta)}{\delta\xi_j\delta\xi_k\delta\xi_l}\Big|_{\xi=0} x_jy_ku_l$ where $i = 1,2$.

Let $p, q \in \mathbb{R}^2$ be two eigenvectors of A for eigenvalue $\lambda_1(\delta_F) = -1$ such that $A(\delta_F)q = -q$ and $A^T(\delta_F)p = -p$. Then we have

$q \sim (2 - d\delta_F + \beta\delta_F x^*, -\beta\delta_F y^*)^T$and $p \sim (2 - d\delta_F + \beta\delta_F x^*, \alpha\delta_F x^*)^T$.

We use $\langle p, q\rangle = p_1q_1 + p_2q_2$, the standard scalar product in $\mathbb{R}^2$to normalize p, q such that $\langle p, q\rangle = 1$. To

do, we set $p = \gamma_{\mathrm{F}}(2 - d\delta_F + \beta\delta_F x^*, \alpha\delta_F x^*)^T$, where $\gamma_{\mathrm{F}} = \frac{1}{(2-d\delta_F+\beta\delta_F x^*)^2-\alpha\beta\delta_F^2 x^* y^*}$.

The sign of the coefficient of critical normal form$l_1(\delta_F)$ determines the direction of the flip bifurcation and is obtained as

$$l_1(\delta_F) = \frac{1}{6}\langle p, C(q,q,q)\rangle - \frac{1}{2}\langle p, B(q,(A-I)^{-1}B(q,q))\rangle \tag{10}$$

We state the following result on direction and stability of flip bifurcation according to above analysis.

Theorem 3.1 *If (7) holds,* $l_1(\delta_F) \neq 0$ *and the parameter* δ *changes its value in a small vicinity of* $FB^1_{E_2}$*, then system (3) undergoes a flip bifurcation around*$E_2(x^*, y^*)$*. Moreover, if* $l_1(\delta_F) > 0$ *(resp.,* $l_1(\delta_F) < 0$*) then the period-2 orbits that bifurcate from* $E_2(x^*, y^*)$ *are stable (resp., unstable).*

3.2 Neimark-Sacker bifurcation

Next, we take parameter $(r, K, \alpha, \beta, d, \delta)$arbitrarily locate in NSB_{E_2}. We consider system (3) at fixed point $E_2(x^*, y^*)$. Then the roots (eigenvalues) of equation (6), are pair of complex conjugate and given by $\lambda, \bar{\lambda} = \frac{-p(\delta)\pm i\sqrt{4q(\delta)-p(\delta)^2}}{2}$.

Let $\delta = \delta_{NS} = -\frac{A_2}{A_1}$ (11)

Therefore, we have$|\lambda| = \sqrt{q(\delta)}$, $q(\delta_{NS}) = 1$. From the transversality condition, we get

$$\frac{d|\lambda(\delta)|}{d\delta}\Big|_{\delta=\delta_{NS}} = -\frac{A_2}{2} \neq 0 \tag{12}$$

Moreover, nondegenerate condition $p(\delta_{NS}) \neq 0,1$, obviously satisfies

$$\frac{A_2^2}{A_1} \neq 2,3 \tag{13}$$

and we have

$$\lambda^k(\delta_{NS}) \neq 1 \quad \text{for } k = 1,2,3,4 \tag{14}$$

Suppose $q, p \in \mathbb{C}^2$ are two eigenvectors of $A(\delta_{NS})$ and $A^T(\delta_{NS})$ for eigenvalues $\lambda(\delta_{NS})$ and $\bar{\lambda}(\delta_{NS})$ such that

$$A(\delta_{NS})q = \lambda(\delta_{NS})q, \quad A(\delta_{NS})\bar{q} = \bar{\lambda}(\delta_{NS})\bar{q}$$

and

$$A^T(\delta_{NS})p = \bar{\lambda}(\delta_{NS})p, \quad A^T(\delta_{NS})\bar{p} = \lambda(\delta_{NS})\bar{p}.$$

By direct computation we obtain

$q \sim (1 - d\delta_{NS} + \beta\delta_{NS}x^* - \lambda, -\beta\delta_{NS}y^*)^T$ and $p \sim \left(1 - d\delta_{NS} + \beta\delta_{NS}x^* - \bar{\lambda}, \alpha\delta_{NS}x^*\right)^T$.

For normalization of vectors p and q, we set $p = \gamma_{\mathrm{NS}}\left(1 - d\delta_{NS} + \beta\delta_{NS}x^* - \bar{\lambda}, \alpha\delta_{NS}x^*\right)^T$, where $\gamma_{\mathrm{NS}} = \frac{1}{(1-d\delta_{NS}+\beta\delta_{NS}x^*-\bar{\lambda})^2-\alpha\beta\delta_{NS}^2 x^* y^*}$.

Then it is clear that $\langle p, q\rangle = 1$ where $\langle p, q\rangle = \bar{p}_1 q_2 + \bar{p}_2 q_1$for $p, q \in \mathbb{C}^2$. Now, we decompose

vector $X \in \mathbb{R}^2$as $X = zq + \bar{z}\bar{q}$, for δ close to δ_{NS} and $z \in \mathbb{C}$. Obviously, $z = \langle p, X\rangle$. Thus, we obtain the following transformed form of system (8) for $|\delta|$ near δ_{NS}:

$$z \mapsto \lambda(\delta)z + g(z, \bar{z}, \delta),$$

where $\lambda(\delta) = (1 + \varphi(\delta))e^{i\theta(\delta)}$ with $\varphi(\delta_{NS}) = 0$ and $g(z, \bar{z}, \delta)$ is a smooth complex-valued function. After Taylor expression of g with respect to $(z, \bar{z})$, we obtain

$$g(z, \bar{z}, \delta) = \sum_{k+l\geq 2} \frac{1}{k!\, l!} g_{kl}(\delta) z^k \bar{z}^l, \quad \text{with} \quad g_{kl} \in \mathbb{C}, \qquad k, l = 0,1, \cdots.$$

According to multilinear symmetric vector functions, the coefficients g_{kl} are

$$g_{20}(\delta_{NS}) = \langle p, B(q, q)\rangle, \quad g_{11}(\delta_{NS}) = \langle p, B(q, \bar{q})\rangle$$
$$g_{02}(\delta_{NS}) = \langle p, B(\bar{q}, \bar{q})\rangle, \quad g_{21}(\delta_{NS}) = \langle p, C(q, q, \bar{q})\rangle,$$

The coefficient $l_2(\delta_{NS})$which determines the direction of NS bifurcation in a generic system exhibiting invariant closed curve can be calculated via

$$l_2(\delta_{NS}) = \mathrm{Re}\left(\frac{e^{-i\theta(\delta_{NS})} g_{21}}{2}\right) - \mathrm{Re}\left(\frac{(1 - 2e^{i\theta(\delta_{NS})})e^{-2i\theta(\delta_{NS})}}{2(1 - e^{i\theta(\delta_{NS})})} g_{20} g_{11}\right) - \frac{1}{2}|g_{11}|^2 - \frac{1}{4}|g_{02}|^2,$$

where $e^{i\theta(\delta_{NS})} = \lambda(\delta_{NS})$.

Summarizing above analysis, we present the following theorem for direction and stability of NS bifurcation.

Theorem 3.2 *If (13) holds, $l_2(\delta_{NS}) \neq 0$ and the parameter δ changes its value in small vicinity of NSB_{E_2}, then system (3) passes through a Neimark-Sacker bifurcation aroundE_2. Moreover, if $l_2(\delta_{NS}) < 0$ (resp.,$>$ 0), then there exists a unique attracting (resp., repelling) invariant closed curve bifurcates from E_2.*

Table 1 Parameter values.

Cases	***Varying parameter in range***	***Fixed parameters***	***System Dynamics***
Case (i)	$1.2 \leq \delta \leq 1.85$	$r = 1.75,\ K = 3.5,\ \alpha = 1.25,\ \beta = 0.25,\ d = 0.25$	FB
Case (ii)	$3.1 \leq \delta \leq 3.42$	$r = 0.75,\ K = 3.5,\ \alpha = 1.25,\ \beta = 0.25,\ d = 0.25$	NS
Case (iii)	$0.22 \leq \beta \leq 0.26$	$r = 0.75,\ K = 3.5,\ \alpha = 1.25,\ d = 0.25,\ \delta = 3.42$	NS

4 Numerical Simulations

In this section, numerical simulation are performed to validate our theoretical results, especially, we present bifurcation diagrams of system (3) around E_2, phase portraits, maximum Lyapunov exponents and fractal dimension corresponding to bifurcation diagrams. We assume that δ is a real bifurcation parameter unless stated. We consider different set of parameter values for bifurcation analysis as given in table 1.

Example 1: Flip bifurcation of system (3) with respect to bifurcation parameter δ.

We set values of parameter as given incase (i). By calculation, we obtain a unique fixed point $E_2(1.0, 1.75387)$ of system (3). The critical point for FB is $\delta_F \sim 1.49096$. It is observed that the system (3) experiences a FB around E_2 when δ passes its critical value δ_F. At $\delta = \delta_F$, the two eigenvalues are $\lambda_1 = -1, \lambda_2 = 0.390811$, $l_1(\delta_F) = 5.765929528187798$ and $(r, K, \alpha, \beta, d, \delta) \in FB^1_{E_2}$. This verifies Theorem 3.1.

The bifurcation diagrams shown in Fig. 1(a-b) reveal that stability of fixed point E_2 happens for $\delta < \delta_F$, at $\delta = \delta_F$ system (3) loses its stability and for $\delta > \delta_F$ there exists a period doubling phenomena leading to chaos. There exists period -2,-4, -8orbits occur at $\delta \sim \{1.4925, 1.694, 1.7655\}$ respectivelyfor the window$\delta \in [1.2, 1.789]$ and chaotic set for $\delta \in [1.789, 1.8435]$. The MLEs and FD related to Fig. 1(a-b) are computed and displayed in Fig. 1(c-d). The status of stable, periodic or chaotic dynamics are compatible with sign of MLE as in Fig. 1(c-d). The phase portraits of bifurcation diagrams in Fig. 2(a-b) for different values of δ are displayed in Fig. 2.

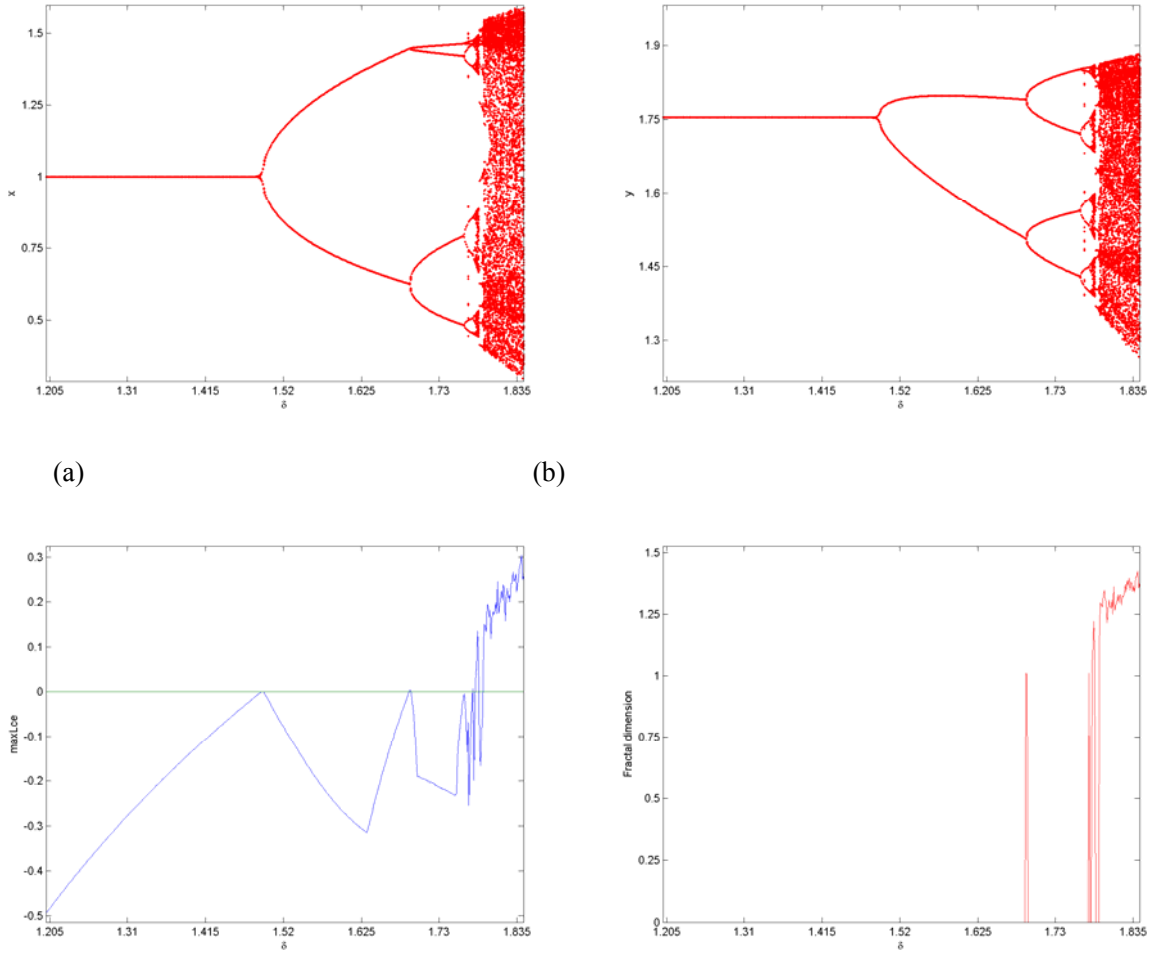

Fig. 1 Flip bifurcation and Lyapunov exponent of system (3) with parameter δ. (a) FB in prey, (b) FB in predator, (c) MLEs related to (a-b), (d) FD corresponding to (a). Initial value $(x_0, y_0) = (0.99, 1.75)$.

Example 2: NS bifurcation of system (3) with respect to bifurcation parameter δ.

With the variation of parameter δ, the system (3) exhibits much richer dynamics through the emergence of NS bifurcation. We take parameters as given in case (ii). After calculation, we find a unique fixed point $E_2(1.0, 0.751658)$. A NS bifurcation point is obtained as$\delta = \delta_{NS}$~3.19294. It isshown that the system (3) experiences a NS bifurcation around E_2 when δ passes its critical value δ_{NS}. Also at $\delta = \delta_{NS}$we have

$$\lambda, \bar{\lambda} = -0.19735 \pm 0.980332\, i,$$

$$g_{20} = -0.4726035296020685 + 0.3977188376549927\, i,$$

$$g_{11} = 0.9557701100152843 - 1.1673536227050705\, i,$$

$$g_{02} = 2.3841437496326363 + 1.9627912980150555\, i,$$

$$g_{21} = 2.8673103300458544 + 3.502060868115212\, i,$$

and $l_2(\delta_{NS}) = -1.6346230671868578$. It is obvious that $(r, K, \alpha, \beta, d, \delta) \in NSB_{E_2}$. This verifies the correctness of Theorem 3.2.

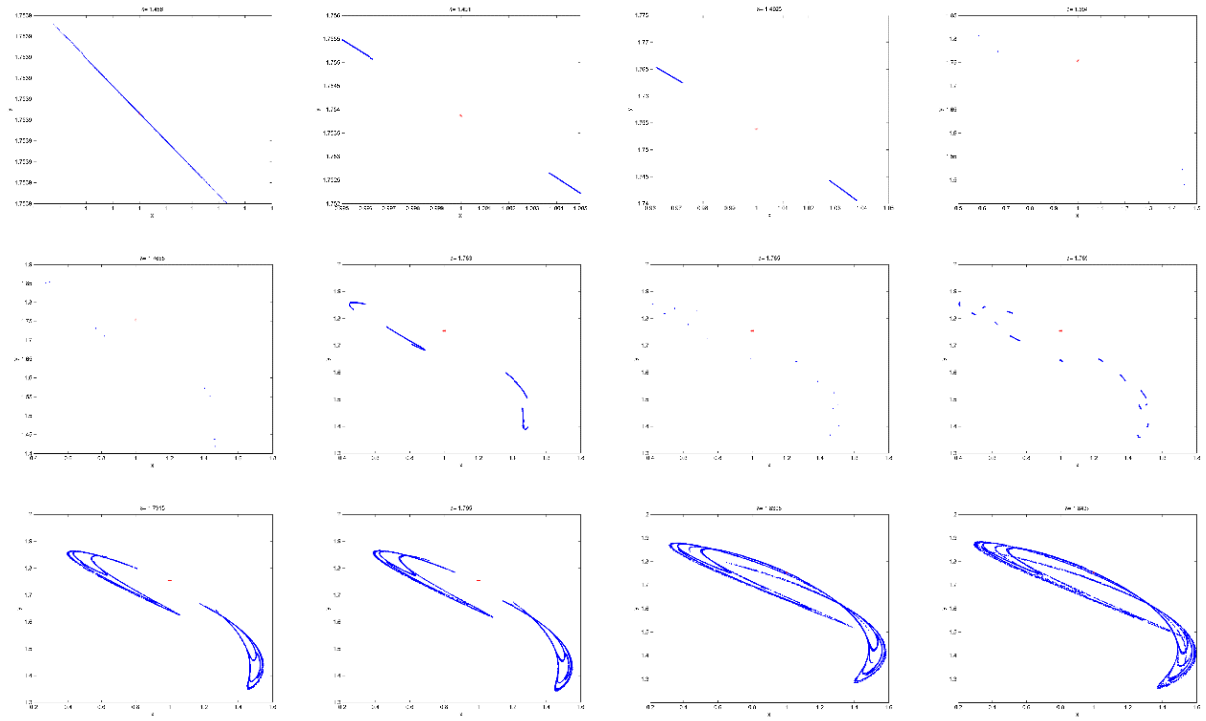

Fig. 2 Phase portraits (xy-plane) of bifurcation diagrams Fig. 1(a-b) for different values of δ.

The bifurcation diagrams shown in Fig. 3(a-b) demonstrate that $E_2$is stabile for$\delta < \delta_{NS}$, loses its stability at $\delta = \delta_{NS}$ and an attracting invariant curve appears if $\delta > \delta_{NS}$. We dispose the MLEs in Fig. 3(c) relating bifurcation in Fig. 3(a-b), which confirm the existences of chaos and periodic orbits as parameter δ varying. These results indicate that NS bifurcation instigates a route to chaos, through a dynamic transition from a stable state, to invariant closed cycle, with periodic and quasi-periodic states occurring in between, to chaotic sets. For instance, when δ~3.42, the sign of MLE confirming presence of chaos.

The phase portraits of bifurcation diagrams in Fig. 3(a-b) for different values of δ are displayed in Fig. 4, which clearly illustrates the act of smooth invariant curve how it bifurcates from the stable fixed point and increases its radius. As δ grows, disappearance of closed curve occurs suddenly and a period-16 orbits appears at $\delta \sim 3.4072$.

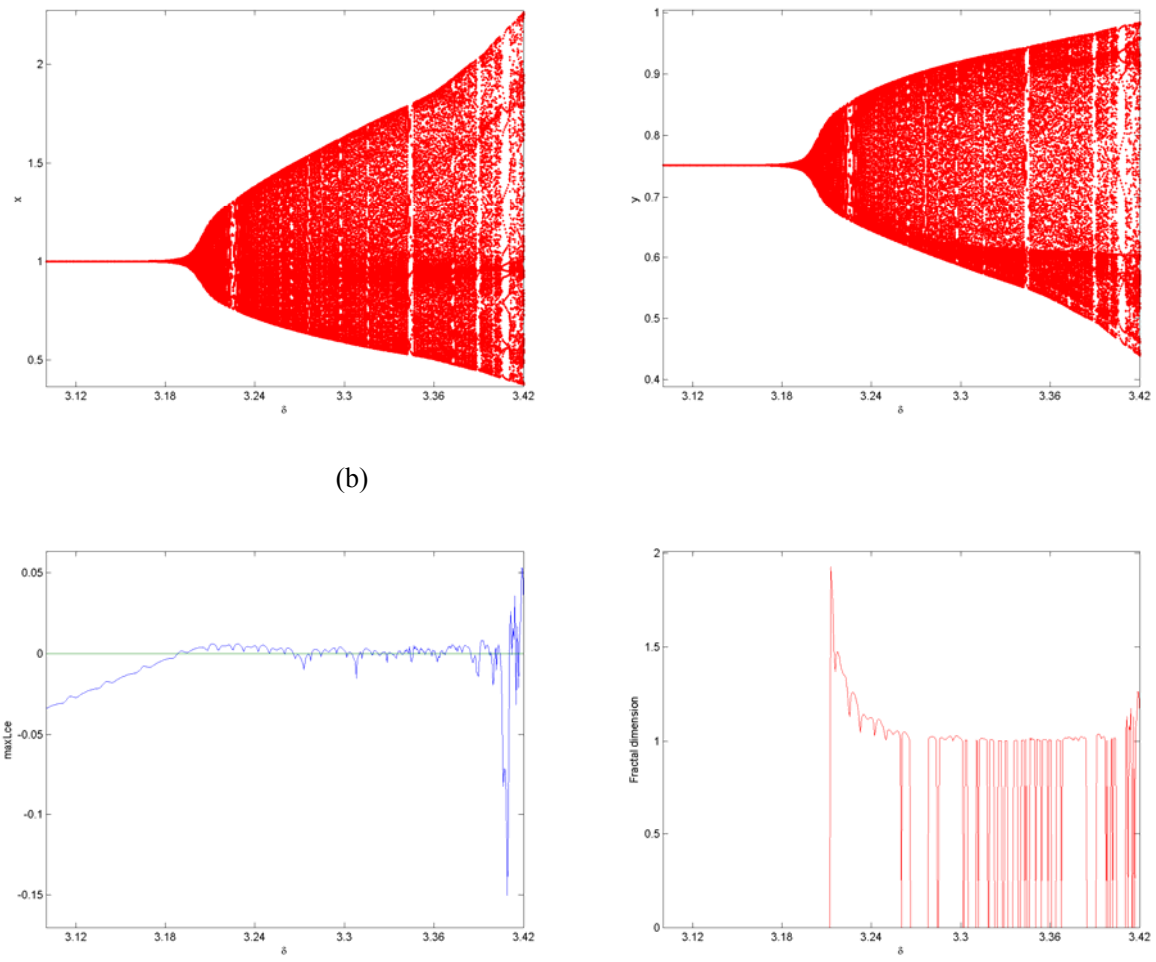

(a) (b)

(c) (d)

Fig. 3 NS bifurcation and Lyapunov exponent of system (3) with parameter δ. (a) NS bifurcation in prey, (b) NS bifurcation in predator, (c) MLEs related to (a-b), (d) FD associated with (a). Initial value $(x_0, y_0) = (0.99, 0.75)$.

Example 3: NS bifurcation of system (3) with respect to bifurcation parameter β.

With the variation of other parameter values (e.g., parameter β), the predator-prey system (3) may exhibit another richer dynamical behaviors. Consider the parameter values as given in case (iii). After calculation, we find a unique fixed point $E_2(1.0867273640123714, 0.7017553241350036)$. It is shown that the system (3) experiences a NS bifurcation around E_2 (which is disposed in Fig. 5(a-b)) when β passes its critical value β_{NS}. The system firstly shows stable dynamics for small value of β. However, with the increase of β value, the stability of the system changes through a NS bifurcation occurring at $\beta = \beta_{NS} \sim 0.2300485$. different nonlinear characteristics to compared Figures 3 and 4 are found in this case, such as route to chaos, invariant curves, chaotic attractors, periodic and quasi-periodic states. The MLE corresponding to Fig. 5(a-b) is

computed and plotted in Fig. 5(c), which confirm the existences of chaos and periodic orbit as parameter β varying. Also at $\beta = \beta_{NS}$we have

$$\lambda, \bar{\lambda} = -0.2824982854378154 \pm 0.9592678034442178\, i,$$
$$g_{20} = -0.6667791365360252 + 0.16041550694510853\, i,$$
$$g_{11} = 1.0090245303587855 - 1.3490208109805368\, i,$$
$$g_{02} = 2.6848281972535943 + 1.6698518248707563\, i,$$
$$g_{21} = 2.785494956066913 + 3.7240825684182757\, i,$$

and $l_2(\delta_{NS}) = -2.168610988511843$.

We notice that system dynamics is stable if $\beta < \beta_{NS}$, loses its stability at $\beta = \beta_{NS}$ and an attracting invariant closed curve appears if $\beta > \beta_{NS}$. That is increased values of parameter β causes complex system dynamics which trigger a route to chaos via NS bifurcation. As βincreases, closed curve suddenly disappear and a period -16, -19, -22, -24, and -14 orbits and attracting chaotic sets appear at $\beta \sim \{0.2444, 0.2472, 0.2488, 0.2564, 0.2584, 0.26\}$ respectively.

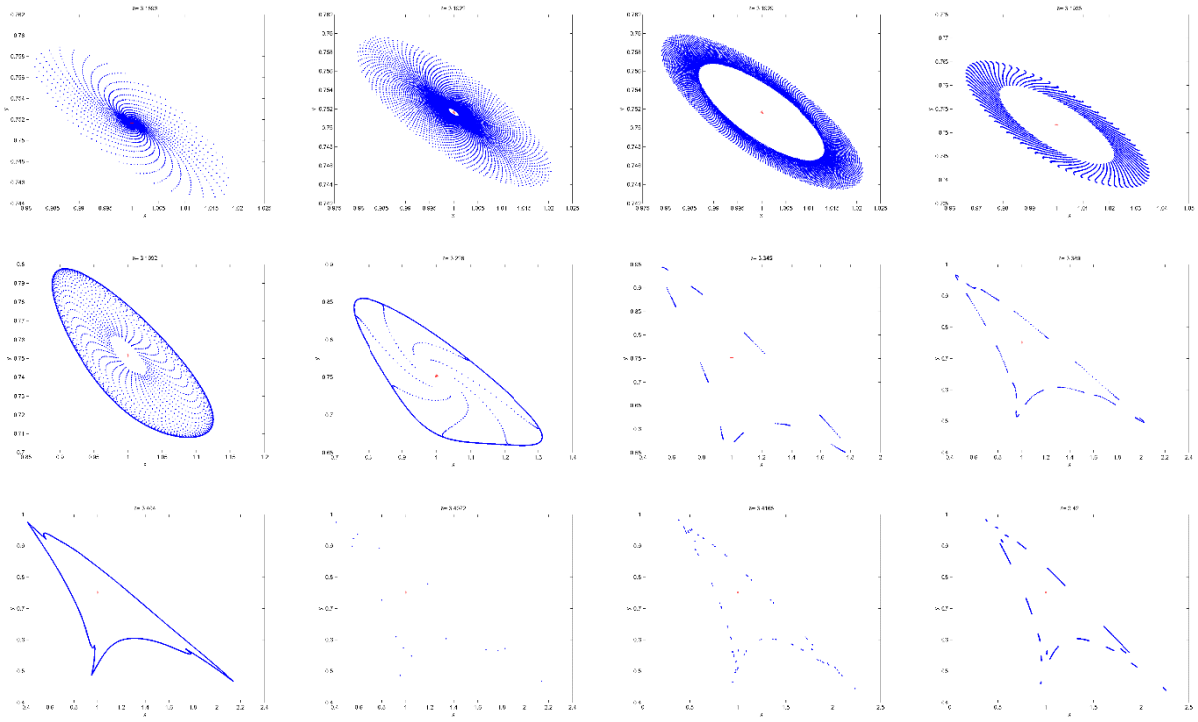

Fig. 4 Phase portraits (xy-plane) of bifurcation diagrams Fig. 3(a-b) for different values of δ.

Example 4: Parametric basins of attractions.

The system (3) may exhibit more complex dynamic behavior when two more parameters change through its critical values. Ina 2D parameter space the parametric basins of attraction (Gkana, 2013) is plotted to notice how the system dynamics qualitatively change as parameter values increase. This plot (Fig. 7) is a numerical analysis tool in which the different colors describe different stability states. So, we plot the parametric basins

of attraction for the parameter values $\delta \in [3.1, 3.42]$ and $\beta \in [0.22, 0.28]$ and rest of parameter values as in case (ii).It is simple to find values of control parameters for which the dynamics of system (3) is in status of non-chaotic, periodic or chaotic. The red and blue regions for an attracting fixed point and/or for stable periodic cycles. The white region corresponds to those parameters values for which the solution trajectories may be quasi-periodic (invariant curves) or non-periodic (chaos, strange attractors). The black region is the set of parameters for which the solution trajectories diverge to infinity.

From 2D parameter space (Fig. 7) we observe that the increases values of control parameters δ and β, the system dynamics significantly change from non-chaotic to chaotic states, i.e., the behaviors of system (3) change from non-periodic to an attracting fixed point or stable periodic cycle.

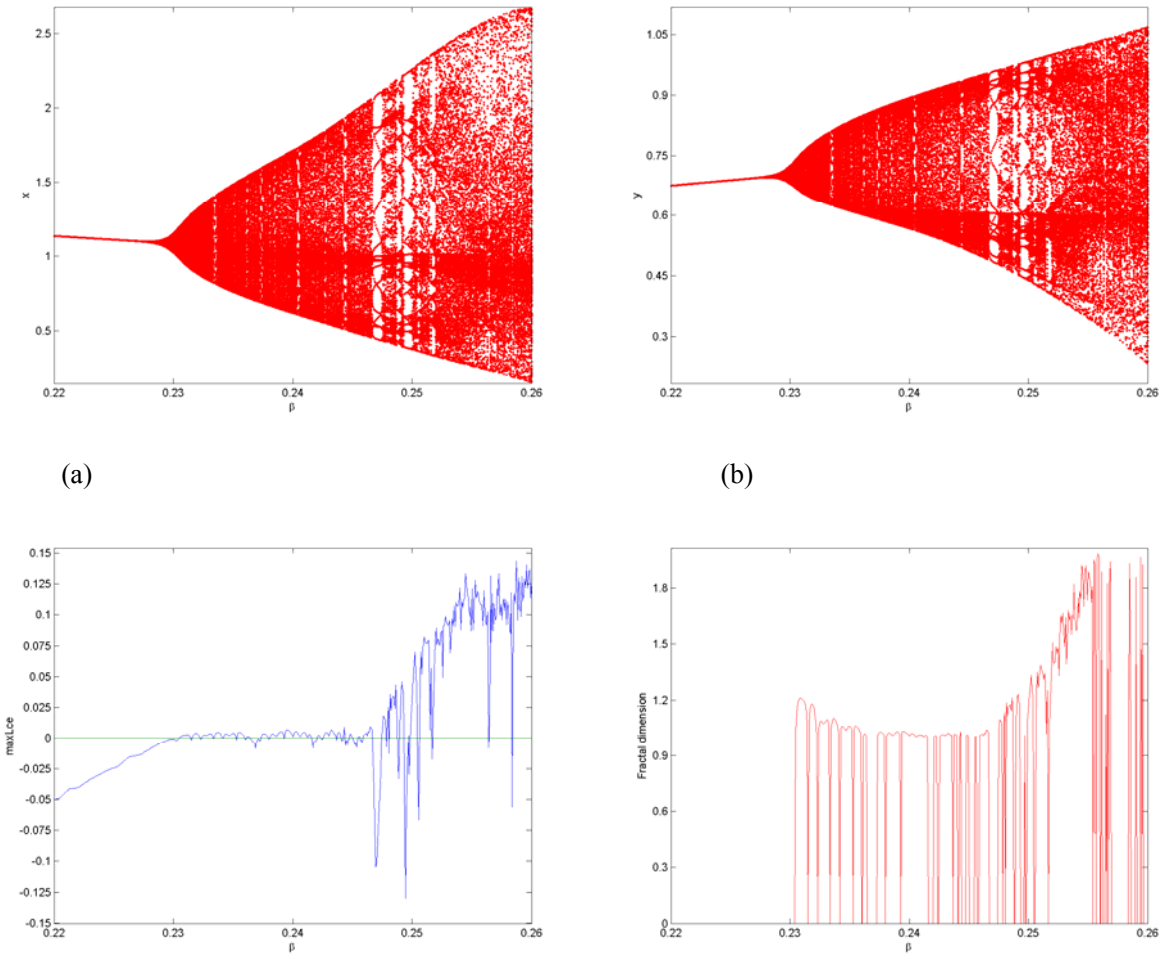

(a) (b)

(c) (d)

Fig. 5 NS bifurcation and Lyapunov exponent of system (3) with parameter β. (a) NS bifurcation in prey, (b) NS bifurcation in predator, (c) MLEs related to (a-b), (d) FD associated with (a). Initial value $(x_0, y_0) = (0.17, 2.11)$.

The measure of fractal dimensions characterizes the strange attractors of a system. By using Lyapunov exponents, the fractal dimension (Cartwright, 1999; Kaplan and Yorke, 1979) is defined by

$$d_L = j + \frac{\sum_{i=1}^{j} h_i}{|h_j|}$$

where $h_1, h_2, \ldots, h_n$ are Lyapunov exponents and j is the largest integer such that $\sum_{i=1}^{j} h_i \geq 0$ and $\sum_{i=1}^{j+1} h_i < 0$.

For our two-dimensional system (3), the fractal dimension takes the form

$$d_L = 1 + \frac{h_1}{|h_2|}, \quad h_1 > 0 > h_2 \text{and } h_1 + h_2 < 0.$$

With parameter values as in Table 1, the fractal dimension of system (3) is plotted in Fig. 1(d), 2(d) and 3(d). The strange attractors given in these figures and its corresponding FD illustrate that the increase values of parameter δ and β cause a chaotic dynamics for the predator-prey system (3).

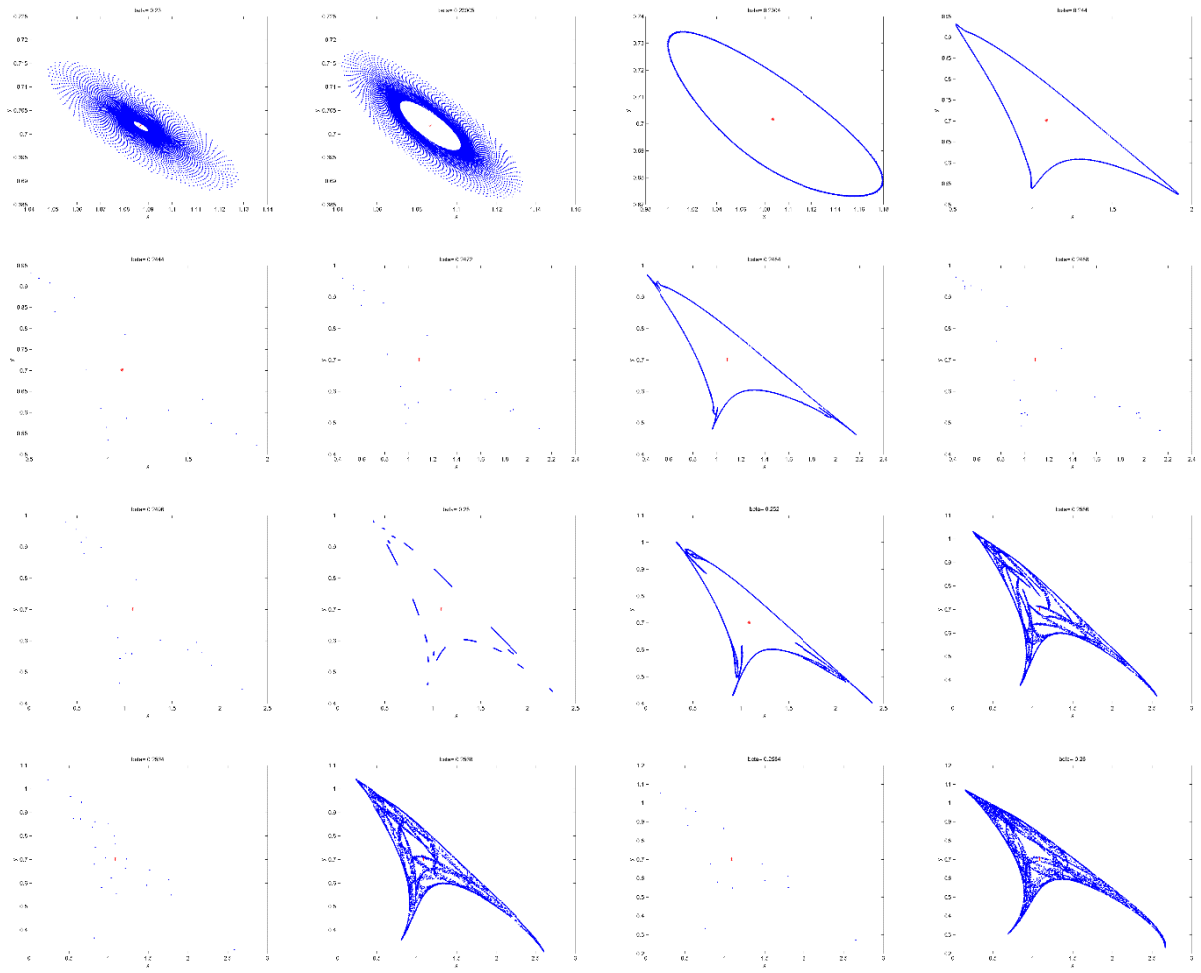

Fig. 6 Phase portraits (xy-plane) of bifurcation diagrams Fig. 3(a-b) for different values of β.

5 Chaos Control

To stabilize chaos at the state of unstable trajectories of system (3), a state feedback control method (Elaydi, 1996) is applied. By adding a feedback control law as the control force u_n to system (3), the controlled form of system (3) becomes

$$\begin{aligned} x_{n+1} &= x_n + \delta\left[r x_n \ln\left(\frac{K}{x_n}\right) - \alpha x_n y_n\right] + u_n \\ y_{n+1} &= y_n + \delta[\beta x_n y_n - d y_n] \end{aligned} \tag{15}$$

and

$u_n = -k_1(x_n - x^*) - k_2(y_n - y^*)$ where $k_1$and k_2 are the feedback gains and (x^*, y^*) represent positive fixed point of system (3).The Jacobian matrix J_c of the controlled system(15) is given by

$$J_c(x^*, y^*) = \begin{pmatrix} j_{11} - k_1 & j_{12} - k_2 \\ j_{21} & j_{22} \end{pmatrix} \quad (16)$$

where $j_{pq}, p, q = 1,2$ given in (5) are evaluated at (x^*, y^*). The characteristic equation of (16) is

$$\lambda^2 - (trJ_c)\lambda + detJ_c = 0 \quad (17)$$

where $trJ_c = j_{11} + j_{22} - k_1$ and $detJ_c = j_{22}(j_{11} - k_1) - j_{21}(j_{12} - k_2)$. Let λ_1 and λ_2 be the roots of (17). Then

$$\lambda_1 + \lambda_2 = j_{11} + j_{22} - k_1 \quad (18)$$

and

$$\lambda_1\lambda_2 = j_{22}(j_{11} - k_1) - j_{21}(j_{12} - k_2) \quad (19)$$

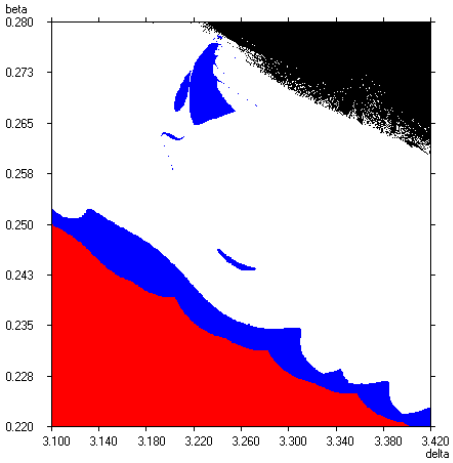

Fig. 7 Diagnostic of system (3) in a 2D parameter space.(a) parametric basins of attraction in (δ, β)-plane.

The solution of the equations $\lambda_1 = \pm 1$ and $\lambda_1\lambda_2 = 1$ determines the lines of marginal stability. These conditions confirm that $|\lambda_{1,2}| < 1$. Suppose that $\lambda_1\lambda_2 = 1$, then from (19) we have

$$l_1: j_{22}k_1 - j_{21}k_2 = j_{11}j_{22} - j_{12}j_{21} - 1.$$

Assume that $\lambda_1 = 1$, then from (18) and (19) we get

$$l_2: (1 - j_{22})k_1 + j_{21}k_2 = j_{11} + j_{22} - 1 - j_{11}j_{22} + j_{12}a_{21}.$$

Next, assume that $\lambda_1 = -1$, then from (18) and (19) we obtain

$$l_3: (1 + j_{22})k_1 - j_{21}k_2 = j_{11} + j_{22} + 1 + j_{11}j_{22} - j_{12}j_{21}.$$

We determine a triangular region in the (k_1, k_2)-plane by plotting the lines $l_1, l_2,$and l_3 (see Fig. 8(a)) which keeps eigenvalues with magnitude less than 1. In order to check how the implementation of feedback control method works and controls chaos at unstable trajectories, we have carried out numerical simulations. With fixed $\delta = 3.42$ and rest parameters as in case (ii), we consider the feedback gains are as$k_1 = 0.1$ and $k_2 = -2.1$. The initial value is $(x_0, y_0) = (0.99, 0.75)$ and Fig. 8(b) and 8(c) show that at the fixed

point $(1.0, 0.751658)$, the chaotic trajectory is stabilized.

6 Discussion

This work is concerned with the dynamics of a discrete-time predator-prey system with Holling type I functional response and Gompertz growth of prey population in the closed first quadrant $\mathbb{R}^2_+$. We determine the existence condition and direction of flip and NS bifurcations of system (3) around E_2 by using the center manifold theory. In particular, we show that at unique fixed point E_2 the system (3) can undergo a flip and NS bifurcation if δ varies around the sets $FB^1_{E_2}$ or $FB^2_{E_2}$ and NSB_{E_2}. Based on Figures, we notice that the small integral step sizeδ can stabilize the dynamical system (3), but the large integral step size may destabilize the system producing more complex dynamical behaviors. In addition, we see that the appropriate choice of the

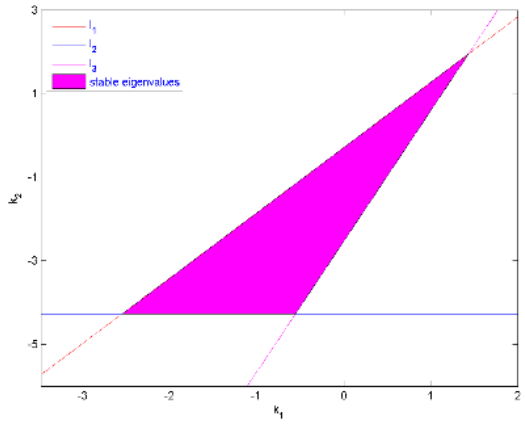

(a)

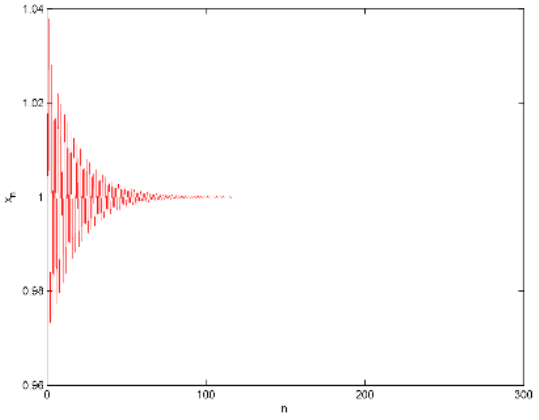

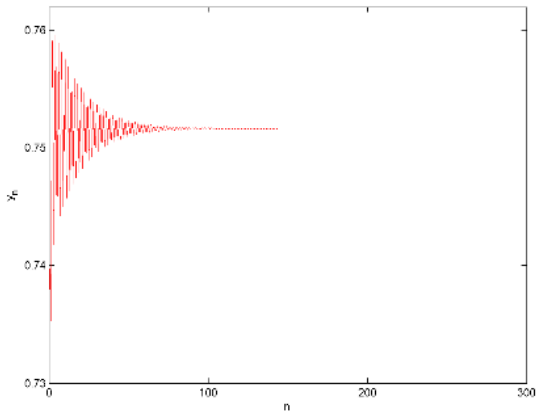

(b) (c)

Fig. 8 Control of chaotic trajectories of system (15). (a) Stability region in (k_1, k_2) plane (b-c) Time series for states x and y respectively.

parameter β(conversion rate of predator) can stabilize the dynamical system (3). However, the high values of β destabilize system (3).Numerical simulations present unpredictable behaviors of the system through a flip bifurcation which include orbits of period -2, -4, -8 orbits and through a NS bifurcation which include an

invariant cycle, orbits of period -14, -16, -19, -22, and period -24orbits and chaotic sets respectively. These indicate that at the state of chaos, the system is unstable and particularly, the predator goes to extinct or goes to a stable fixed point when the dynamic of prey is chaotic. We compute MLEs and FD for justification about the existence of chaos. The two bifurcations (FB and NSB) both trigger a route to chaos via periodic and quasi-periodic states; that is, chaotic dynamics appear or disappear along with the emergence of bifurcations. Moreover, we plot the parametric basins of attraction for system (3) by the variation of two control parameters which shows very rich nonlinear dynamical behaviors and so one can directly observe from the 2D parametric spaces when the system dynamics will be periodic, quasi-periodic and chaotic. Finally, the chaotic trajectories at unstable state are controlled by implementing the strategy of feedback control.

References

Berryman AA. 1992. The origins and evolution of predator-prey theory. Ecology, 73: 1530-1535

Cartwright JHE. 1999. Nonlinear stiffness Lyapunov exponents and attractor dimension. Physics Letters A., 264: 298-304

Elaydi SN. 1996. An Introduction to Difference Equations. Springer-Verlag, New York, USA

Freedman HI. 1980. Deterministic Mathematical Models in Population Ecology, Marcel Dekker, New York, USA

Gkana A, Zachilas L. 2013. Incorporating prey refuge in a prey–predator model with a Holling type I functional response random dynamics and population outbreaks. Journal of Biological Physics, 39: 587-606

Gompertz B. 1825. On the nature of the function expressive of the law of human mortality etc. Philosophical Transactions of Royal Society. 115: 513-585

He ZM, Lai X. 2011. Bifurcation and chaotic behavior of a discrete-time predator-prey system. Nonlinear Analalysis and Real World Applications, 12: 403-417

He ZM, Li Bo. 2014. Complex dynamic behavior of a discrete-time predator-prey system of Holling-III type. Advances in Differential Equations, 180

Kaplan JL, Yorke YA. 1979. A regime observed in a fluid flow model of Lorenz. Communications in Mathematical Physics, 67: 93-108

Kuzenetsov YA. 1998. Elements of Applied Bifurcation Theory (2nd Ed). Springer-Verlag, New York, USA

Liu W, Cai D. 2019. Bifurcation, chaos analysis and control in a discrete-time predator-prey system. Advances in Differential Equations, 11

May RM. 1974. Stability and Complexity in Model Ecosystems. Princeton University Press, USA

Rana SMS. 2015. Bifurcation and complex dynamics of a discrete-time predator-prey system with simplified Monod-Haldane functional response. Advances in Differential Equations, 345

Rana SMS, Kulsum U. 2017. Bifurcation analysis and chaos control in a discrete-time Predator-Prey System of Leslie Type with Simplified Holling Type IV Functional Response. Discrete Dynamics in Nature and Society, 2: 1-11

Rana SMS. 2019. Bifurcations and chaos control in a discrete-time predator-prey system of Leslie type. Journal of Applied Analysis and Computation, 9(1): 31-44

Rana SMS. 2019. Dynamics and chaos control in a discrete-time Holling-Tanner model. Journal of the Egyptian Mathematical Society, 27: 48

Zhao M, Li C, Wang J. 2017. Complex dynamic behaviors of a discrete-time predator-prey system. Journal of Applied Analysis and Computation, 7: 478-500

Zhao M, Xuan Z, Li C. 2016. Dynamics of a discrete-time predator-prey system. Advances in Differential Equations, 191